SCIENCE BULLETIN
CHIAO TUNG UNIVERSITY
Vol. 5, No. 1 , APRIL 1971

Charge Transport and Storage Effect of Gold Ion Implanted Silicon Dioxide MOS Structure

L. I. CHEN, and S. M. SZE *

College of Engineering, National Chiao Tung University

Hsinchu, Taiwan, Republic of China

Abstract

When gold ions of sufficiently high dose ($\sim 10^{14}$ ions/cm^2) are implanted into thermally grown silicon dioxide MOS structure, novel charge transport and memory effect have been observed. For a typical structure with 800 Å SiO_2 and a projected ion range of 400 Å, most of the induced interface states can be annealed out at 400°C. The charge transport in the implanted oxide is found to follow the Frenkel-Poole emission process with trapping energy level at 1.21 eV from the conduction band.

Since the charge transport in the inner part of the oxide is by the Fowler-Nordheim tunneling mechanism, the MOS structure is equivalent to a double-layer memory device in which charges can be stored at the trapping centers inside the oxide when voltges are applied. Effects of oxide thickness, ion dose level, annealing temperature, and measurement temperature have been studied. Good agreements have been obtained between experimental results and theoretical predictions.

I. Introduction

Recently, the mechanism of transport and storage effects of electric charges in thin insulating films has been increasingly investigated. It has been shown[1-5] that charges can be stored at the interface between two thin insulating layers because of the different charge transport mechanisms through the two layers. The structure will then show a hysteresis effect and can act as a memory. In order to have a good memory effect, the density of the insulator-insulator interface states used for storing charges must be large. This can be achieved by using a metal layer[1] or by the natural disorder states between the insulating layers[2-5].

It has been shown[6] that O^+ and Ne^+ implantation on thermally oxidized silicon create deep trapping states in the interface region. In this experiment heavy ions are implanted into a thermal oxide to form ion induced trapping centers at the ion projected range (distance from oxide

* Prefessor at Large, College of Engineering, National Chiao Tung University

Present Address: Bell Telephone Laboratories, [redacted] Murray Hill, New Jersey, U. S. A.

surface to the peak of the implanted ion distribution). The concentration of the ion induced trapping centers will be high because of the small ion projected straggling due to heavy ions. The damage in outer part of the oxide caused by heavy implanted ion will affect the charge transport mechanism of that region. These effects will provide the storage of charges in the oxide and therefore show a hysteresis effect. In this work, gold ions are chosen to study this possibility.

The favrication of the MOS structure with gold ion implanted oxide is described in Section II. The distribution function of gold ion in SiO_2 is given in Section III. The effects of the ion doses, the annealing temperatures and the measuring frequencies on the MOS capacitance characteristics are shown and discussed in Sections IV and V. The charge storage and transport mechanism are analyzed in Section VI. Finally a brief discussion and conclusion are given in Section VII.

II. Fabrication of MOS Structure with Gold-Ion Implanted Oxide

The silicon substrates were of 1 ohm-cm and 0.001 ohm-cm n-type, ⟨111⟩ oriented and syton polished on one side. In order to reducing the series resistance effect, the degenerate substrates were chosen for the I-V conduction measurements. Firstly the substrates were performed a preoxidation cleaning and then oxidized in atmosphere steam at 1050°C for thirty minutes. Just before the substrates were loaded into the oxidation oven for the final silicon dioxde layer, they were immersed in hydrofluoric acid for two minutes to remove the pre-oxididation SiO_2 layer, then rinsed in deionized water. At this point the silicon wafers were completely hydrophobic, thus no drying of the wafers was necessary. The substrates were oxidized in an oven using a quartz reactor tube and a silicon carbide liner at 950°C in atmospheric steam. Immediately after oxidation the wafers were scribed and broken in half. On one-half of the wafer, aluminum was evaporated from a sodium free tungsten filament through a molydenum mask hole onto the silicon wafer on which an array of dots with 2000Å in thickness and 5 mils in diameter were made. This half of the wafer acted as the "control". A small space on the control which was free of aluminum dots was used for ellipsometer measurements to determine oxide thickness. To ensure back ohmic contacts the substrate were liquid honed, cleaned, and degreased. Finally, aluminum films of 3000Å thick were evaporated from a sodium free tungsten filament on the back side without alloying.

Gold impurity ions were implanted at room temperature using a mass-analysed, 100 KeV, Au^+ beam into the other half of thermally oxided silicon wafer. The ion currents varied for different implants from 2×10^{-8} to 10^{-6} Amp. As secondary electrons from the target are reflected back from a screen electrode, measured doses were accurate to 1%. The beam is scanned in both vertical and horizontal directions to give a uniform impurity concertration scross the slice. Deviations from uniformity are estimated as less than 1%. The beam source material is dried $AuCl_3$

crystals placed in the r.f. accelerator source chamber. After gold ion implantation the aluminum dots and back contacts were formed with the same process as that of the control.

All samples were annealed with Al contacts at 200°C, 300°C, and 400°C for 30 minutes in dry nitrogen gas with liquid nitrogen as a cold trap.

III. Gold Ion Distribution in SiO_2

The gold ion distribution $n(s, R_p, \Delta R_p)$ in the SiO_2 film is assumed to be a Gaussian function,

$$n(x, R_p, \Delta R_p) = \frac{\phi}{\sqrt{2\pi}\Delta R_p} \exp -\left(\frac{x-R_p}{\sqrt{2}\Delta R_p}\right)^2 \qquad (1)$$

Here ϕ is the dose; R_p, the projected range; ΔR_p, the projected stragging; and x, the depth. For Au^+ ion with 100 KeV energy we take[7] $R_p = 380\text{Å}$ and $\Delta R_p = 86\text{Å}$.

The number of ions which pass through the interface of an oxide of thickness d into the substrate may be obtained from

$$N(d) = \int_d^\infty n(x)\, dx = \frac{\phi}{2} \operatorname{erfc}\left(\frac{d-R_p}{\sqrt{2}\Delta R_p}\right) \qquad (2)$$

where erfc is the complementary error function.

IV. Effects of Implanted Dose and Annealing Temperature on MOS Capacitance Characteristics

Gold ions were implanted with an ion energy of 100 KeV and for three different doses of 10^{12}, 10^{13}, and 10^{14} cm^{-2}. The capacitance-voltage (C-V) curves of the implanted and the control sample were measured at a frequency of 1 MHz.

Consider the control as ideal MOS diodes, the flat-band capacitance of the control with silicon substrate of 1 ohm-cm and oxide thickness of 750Å is $0.8\, C_{ox}$,[8] where C_{ox} is the oxide capacitance. The corresponding voltage is defined as flat-band voltage. For the convenience of discussion, an effective flat-band voltage shift ΔV_{FB} between the implanted and the control was defined as the difference of voltages where the capacitances equal to $0.8\, C_{ox}$. The sign of ΔV_{FB} is positive when the effective flat-band voltage of the implanted sample is more positive than that of the control.

Since the C-V characteristics of the implanted sample depend on the applied high field, small voltage which is large enough to cover the MOS capacitance from inversion to accumulation region was used. In some cases the C-V curves were shifted due to high field, then a propriety

voltage with opposite polarity was applied to cause the C-V curves returning to their original positions.

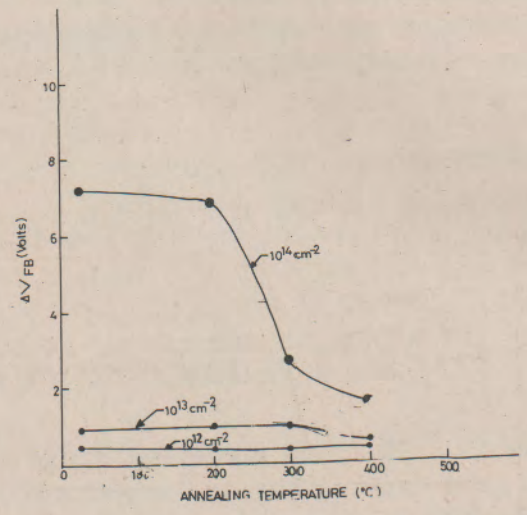

Fig. 1. Effective flatband voltage shift as a function of annealing temperature for 30 minutes in dry nitrogen with liquid nitrogen as a cold trap. The implanted gold ion doses are 10^{12}, 10^{13} and 10^{14} cm^{-2} implanted at 100KeV. The oxide thickness is 750Å. The measurement frequency is 1 MHz.

The effects of implanted dose and annealing temperature on the effective flat-band voltage shift is shown in Fig. 1. The oxide thickness before gold implantation is 750Å. The effective flat-band voltage shift is shown to be increased with increasing gold ion dose. This indicates that the gold ions and the damage caused by the gold implantation do enhance the density of trapping centers at Si-SiO_2 interface and/or in the oxide. For the dose of 10^{12} cm^{-2} and 10^{13} cm^{-2} the effective flat-band voltage shifts are 0.5 and 1 Volt respectively, and remain unchanged when were annealed at temperatures up to 400°C. For the sample of 10^{14} cm^{-2} dose, the effective flat-band voltage shift is 7 Volts before annealing and largely drops down to 2.5V after annealing in dry nitrogen at 300°C for 30 minutes, and remains almost constant arround and above 400°C annealing. However, it did not try for annealing higher than 400°C, because the diffusion of gold ions at such temperatures can not be neglected.

Fig. 2 shows the C-V curves of another 10^{14} cm^{-2} gold ions implanted sample. The thickness of the oxide before implantation is 720Å, which is 30Å thinner than the sample shown in Fig. 1. By comparing Fig. 1 with Fig. 2 it is obvious that the effective flat-band voltage shifts depend stronly on the thickness of the oxide. Since they have the same gold ion dose implanted at same ion energy, the large difference in the effective flat-band voltage indicates that the induced interface states must depend strongly on the oxide thickness. For the sample without

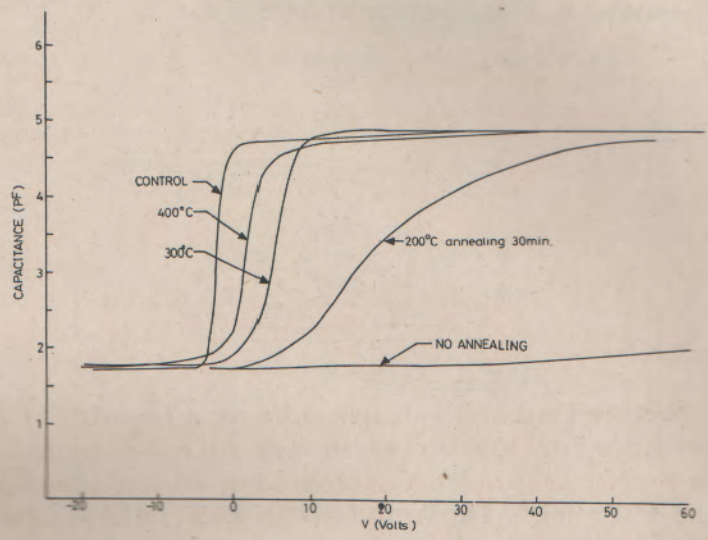

Fig. 2. MOS capacitance vs. voltage applied at the metal under different annealing conditions. The gold ion dose is $10^{14}cm^{-2}$. The oxide thickness is 720 Å.

annealing, the MOS capacitance shown in Fig. 2 is always of the inversion region within the measuring voltage up to the breakdown voltage range. When it was annealed at 200°C for 30 minutes, the I-V curve is still largely distorted from the ideal one due to large amount of fast surface states. The effective flat-band voltage shift again drops largely after 300°C annealing, and the C-V curve becomes only slightly distorted compared with that of 200°C annealed sample. Most of the fast surface states have been eliminated after 400°C annealing for 30 minutes. The remained effective flat-band voltage shift ΔV_{FB} might be to due to the charged deep trapping centers of implanted gold ions in the oxide. Since ΔV_{FB} is positive, the deep trapping centers are mainly of acceptor type.

V. Effect of Frequency on Capacitance Characteristics

The fast interfact states induced by gold ion implantation into a thermally grown oxide can be well demonstrated by measuring C-V curves at various frequencies. Fig. 3 and Fig. 4 show the effect of frequencies

on MOS capacitances. The oxide film thickness is 720Å, and was implanted by gold ions at 100 KeV with a dose of 10^{14} cm^{-2}, and then annealed in dry nitrogen for 30 minutes at 200°C and 400°C respectively. From the highly distorted and splitted C-V curves in Fig. 3 it is obvious that there still have a lot of interface states after 200°C dry nitrogen annealing for 30 minutes. Most of these interface states can be eliminated when the annealing temperature increases to 400°C as is shown in Fig. 4

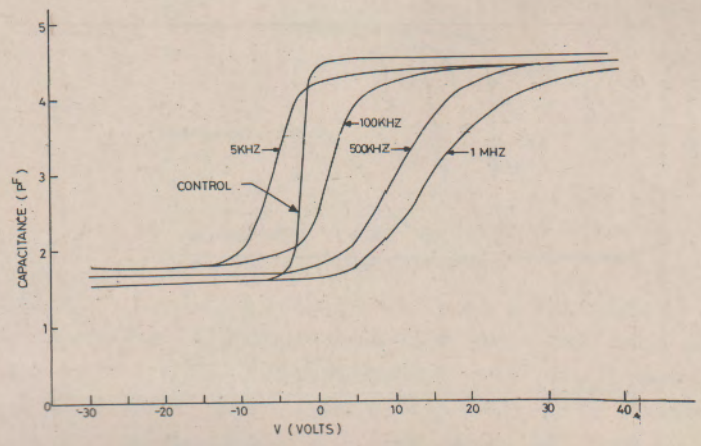

Fig. 3. MOS capacitance vs. voltage for different measuring frequencies. The sample is same as that of Fig. 2 but annealed at 200°C for 30 minutes in dry nitrogen.

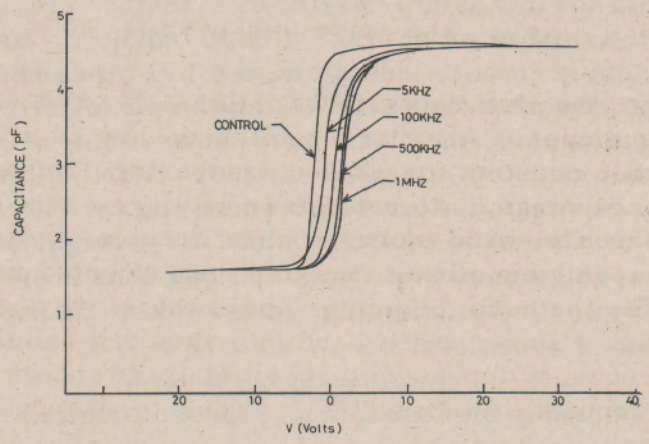

Fig. 4. MOS capacitance vs. voltage for different measuring frequencies. The sample is annealed at 400°C for 30 minutes in dry nitrogen.

In Fig. 1 and Fig. 2 it has been shown that the gold implantation induced interface states depend strongly on the thickness of the oxide. The interface states will increase drastically with small decrease of the oxide thickness, and can mostly be eliminated at 400°C dry nitrogen annealing for 30 minutes. In order to investigate the thickness and the annealing effect on the interface states by measuring the MOS capacitances at various frequencies, an MOS structure with SiO_2 of 400Å thick was implanted by gold ion at 100 KeV to a dose of 10^{14} cm^{-2}. The sample was then annealed at 400°C in dry nitrogen for 30 minutes.

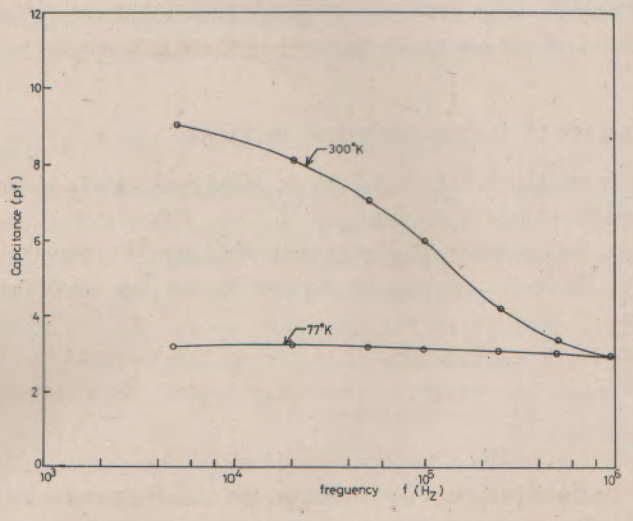

Fig. 5. MOS capacitance measured at various frequencies. At a fixed measuring frequency, the capacitance is in the deep inversion region and remain constant within the measuring voltage range up to breakdown voltage. The gold ion dose in 10^{14} cm^{-2} implanted at 100KeV. The oxide thickness is 400Å

Fig. 5 shows the MOS capacitance of this 400Å oxide sample measured at various frequencies. All the capacitances are in strong inversion region and remain constant for a fixed measuring frequency within the measuring voltage range up to breakdown voltage. The values of the capacitance decrease with increasing frequencies. Since the oxide thickness (400Å) is very close to the gold ion projected range (380Å) implanted at 100 KeV, the Si-SiO_2 interface is therefore highly damaged by the implanted heavy ions crossing the interface and can no longer be removed. The frequency dependent inversion capacitances can be explained by the lateral current flow effect [9,10] due to charged trapping centers in the oxide and/or the interface charge states on the silicon surface.

The capacitances measured at liquid nitrogen temperature (77°K) are shown in Fig. 5 which are independent of the frequency. This indicates

that the minority carriers cannot follow the frequencies at such low temperature and that the 1 MHz frequency is high enough to measure the room temperature high frequency C-V curves as shown by Fig. 5.

VI. Conduction and Charge Storage in MOS Structure with Gold Ion Implanted Oxide

It has been shown [11] that the transport mechanism of a thermally grown SiO_2 is due to Fowler-Nordheim tunneling. However if the oxide film is implanted by heavy ions, the damage and the trapping centers in the oxide due to implantation might affect the charge transport mechanisms. In this section, the effects of gold ion implantation on the charge transport and storage in an MOS structure with implanted oxide are studied.

1. Current Transport in the Control Sample

The current transport mechanism in thermal oxide is electrode-limited due to Fowler-Nordheim tunneling [11]. Electrons tunnel from the silicon conduction band edge through the triangular barrier into the oxide conduction band. Hole emission is assumed to be negligible because of the high barrier.

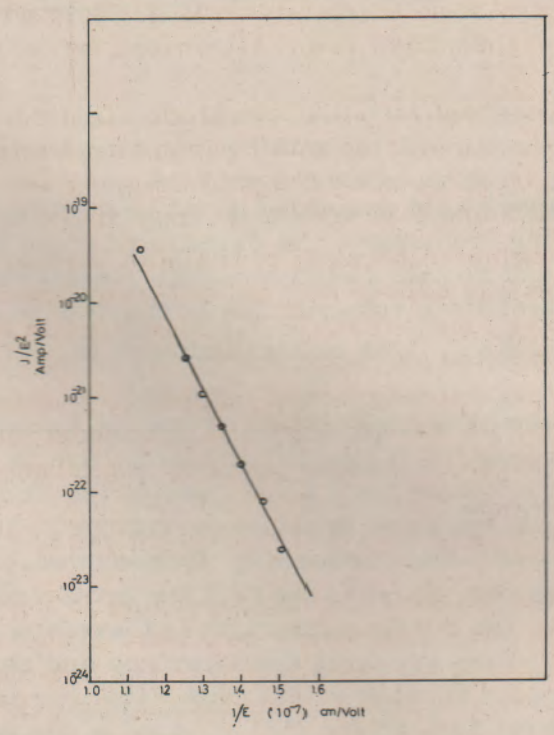

Fig. 6. Current characteristics of control sample plotted in Fowler-Nordheim form. The silicon dioxide was grown in steam at 1050°C. The oxide thickness is 910Å. The aluminum dot is 5 mils in diameter.

For measuring the I-V characteristics of the control, an MOS sample with oxide thickness of 910Å was applied with positive voltage at the aluminum dot which is 5 mils in diameter. The current characteristics was plotted in a Fowler-Nordheim form (J/E^2 vs. $1/E$) and did show a straight line as shown in Fig. 6. By fitting this plot one obtains the following expression:

$$J = C_o E^2 e^{-E_o/E} \qquad (3)$$

where J is current density; E, electric field; $C_o = 10^{-11}$ Amp/V^2; $E_o = 1.755 \times 10^8$ V/cm. This result is in good agreement with that of Lenzlinger and Snow[11] in the interested high field region. The deviation in the low field region might be due to different growing conditions of the oxide film.

2. Current Transport in Ion Implanted Sample

Fig. 7 shows a simple model of the energy band diagram of an MOS structure with positive voltage applied at metal side. The gold ions were implanted to a depth of d_2 from oxide surface and formed a high concentration of trapping centers. The oxide film was then divided into two regions. In region 1, effect of gold ion implantation is neglected, while in region 2, there are some trapping levels due to gold implantation damage though some of them have been eliminated by 400°C annealing for 30 minutes.

In region 1 the current is still electrode-limited due to Fowler-Nordheim tunneling because of the small implantation effect in this region. Electrons will then be trapped by the gold trapping centers at the boundary of regions 1 and 2 and then transport from there to the metal. Hole emission is again neglected because of the high barrier. The transport mechanism in region 2 is expected to be different from that of region 1. It can be determined by measuring D. C. steady-state I-V curves of both control and gold implanted MOS structure.

Because there are trapping levels induced by implantation damage in region 2 of the oxide, we assume that the transport mechanism in this region is due to Frenkel-Poole emission and is expressed by [12]

$$J_2 = C E_2 \exp\left[-\frac{q}{kT} \left(\phi_B - \sqrt{q E_2 / \pi \varepsilon_i} \right) \right] \qquad (4)$$

where C is the characteristic constant depending on the trap level, q the electronic charge, k the Boltzmann's constant, T the absolute temperature ϕ_B the depth of the trapping level, and ε_i the dielectric constant of the insulator. The subscript 2 indicates that the current density J and electric field E are of region 2 only.

At a fixed temperature, Eq.(6) can be rewritten as

$$J_2 = C_2 E_2 \exp\left(C_2' \sqrt{E_2} \right) \qquad (5)$$

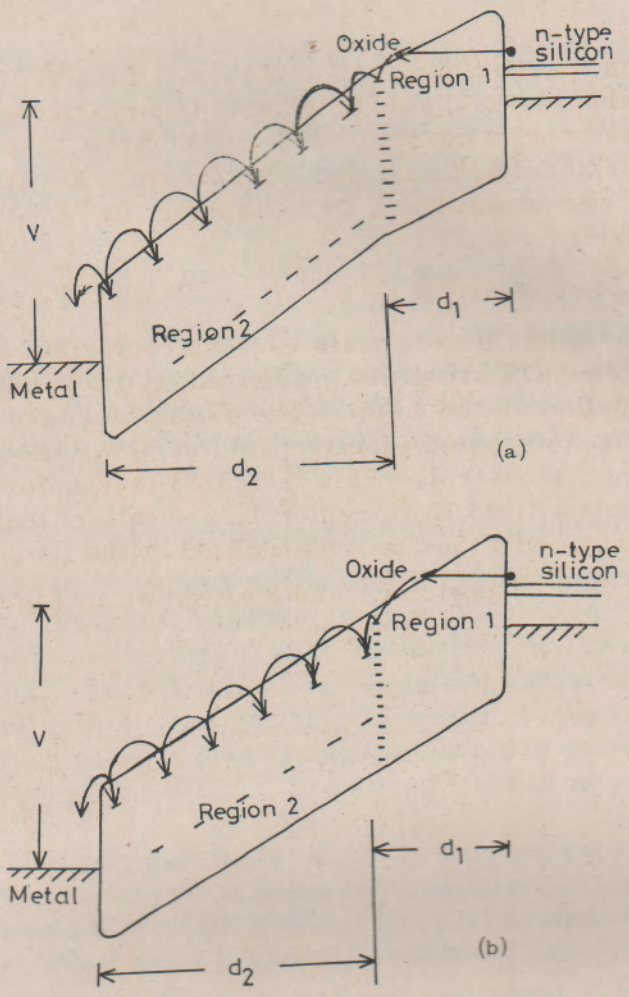

Fig. 7. Simple model of the energy band diagram of gold ion implanted oxide MOS structure with positive voltage applied at the metal. (a) At t=0, the initial charge stored in oxide is zero. (b)Steady state condition.

where

$$C_2 = C \exp\left(-\frac{q}{kT}\phi_B\right) \tag{5A}$$

$$C_2' = \frac{q}{kT}\sqrt{\frac{q}{\pi\varepsilon_1}} \tag{5B}$$

Some assumptions have been made to simplify the problem: (1) The Gaussian ion distribution is approximated by a delta function. (2) The thickness and the dielectric constant of the oxide do not change after gold ion implantation. (3) The effect of interface states is small. (4) The voltage drop in oxide due to charged trapping centers is small.

In order to study the charge transport and storage mechanism of the implanted sample, the MOS samples with oxide film 700Å to 1000Å thick

were implanted by gold ions at 100 KeV to a dose of 10^{14} cm^{-2}, and were finally annealed at 400°C for 30 minutes in dry nitrogen. In measuring the D.C. steady state current each reading was taken after the current dropped to its steady-state value. The storage of charges in oxide trapping centers was investigated by measuring the C-V curves at a frequency of 1 MHz.

A. Steady State Analysis

Fig. 8 shows the steady state I-V characteristics of the gold ion-implanted oxide MOS structure measured at room temperature with positive bias applied on the metal. The oxide thickness is 910Å. It shows that in the most interested electric field region, the conduction is smaller than that of the control. This indicates that under steady state condition the electric field E_1 in region 1 is smaller than E_2 of region 2. Negative charges will thus be accumulated at the trapping centers which form the boundary of regions 1 and 2 as shown in Fig. 6(b).

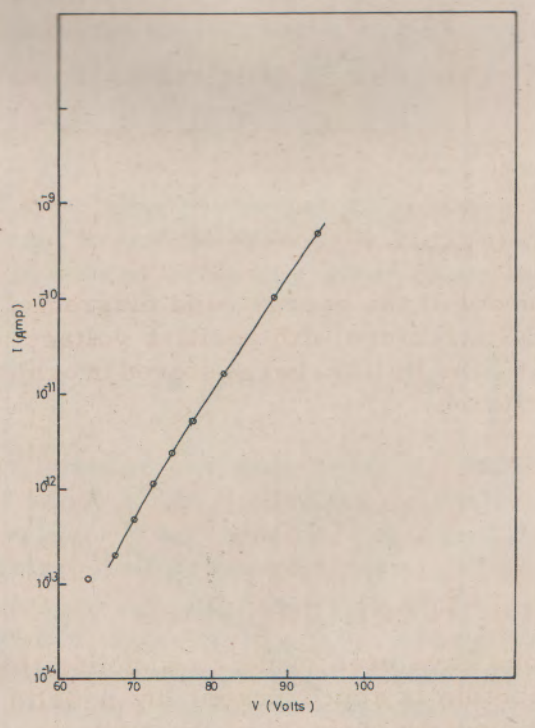

Fig.8. The steady state room temperature I-V characteristics of implanted sample measured at room temperature when positive bias is applied on the metal. The oxide thickness is 910Å, and was implanted by gold ion at 100 KeV to a dose of 10^{14} cm^{-2} The aluminum dot is 5 mils in diameter.

Under the steady state condition, the current densities in regions 1 and 2 are equal

$$J = J_2(E_2) = J_1(E_1) = C_1 E_1^2 e^{-E_o/E_1} \qquad (6)$$

here we have assumed that the transport mechanism in region 1 remains in the form of Fowler-Nordheim tunneling. With the assumption that the voltage drop due to charged trapping centers is negligible, the relation between E_1 and E_2 can be expressed as

$$E_1 d_1 + E_2 d_2 = V \qquad (7)$$

where V is the applied voltage on the metal; d_1 and d_2 are the widths of regions 1 and 2 of gold ion implanted oxide respectively. For 100 KeV gold ion implantation we take $d_2 = R_p + \Delta R_p = 466\text{Å}$ and $d_1 = T_{ox} - d_2$, where T_{ox} is the thickness of the oxide film.

The current transport equation of the implanted oxide in region 2, $J_2(E_2)$ can then be solved by the steady state current characteristics (Fig. 8), Eq.(4)and Eq.(5) The computer solved results of $J_2(E_2)$ was plotted in Frenkel-Poole emission form (i.e. J/E vs $\sqrt{E}$) in Fig. 9 and

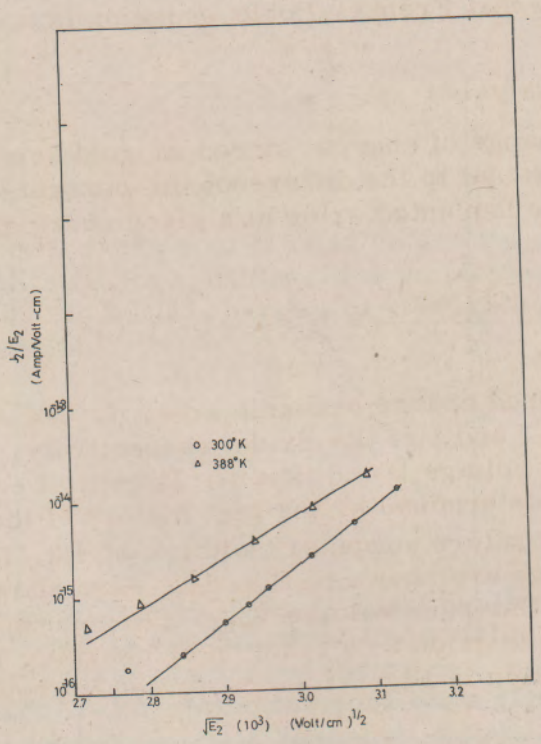

Fig. 9. Current characteristics of implanted sample plotted in Frenkel-Poole for T=300°K and T=388°K.

do show a straight line in the most interested electric field region. However the straight line in the J/E vs $\sqrt{E}$ plot does not uniquely imply a Frenkel-Poole transport mechanism, for Schottky emission also shows a straight line in the same plot. One way to distinguish between Schottky and Frenkel-Poole emissions is by checking the slope of that straight line and then solve the corresponding dielectric constant ε_i by Eq.(5B) If it is due to Frenkel-Poole emission, the value of ε_i should close to ε_{ox} , the dielectric constant of SiO^2 . For the case of Schottky emission, the corresponding value of ε_i solved by Eq.(5B) should close to 4 ε_{ox} [12] . By fitting Eq.(5) to Fig. 9 (take T = 300°K), one obtains $C_2 = 1.98\times10^{-33}$ Amp/cm-Volt, $C_2' = 1.38\times10^{-2}$(cm/Volt)$^{1/2}$, and $\varepsilon_i = 1.1\varepsilon_{ox}$ Therefore one may safely assume that the transport mechanism in region 2 of the implanted oxide is of Frenkel-Poole emission.

To determine the values of C and ϕ_B in Eq. (5A), one has to know another value of C_2 at temperature other than 300°K. Using the same approach as before, $J_2(E_2)$ at 115°C was plotted in Frenkel-Poole form and compares with that of room temperature in Fig. 9. One then obtains $C = 4\times10^{-13}$ Amp/Volt-cm and $\phi_B = 1.21$ Volts.

From Eq.(5B), the slope of straight line in Fig. 9 should reversely proportional to the absolute temperature if it is due to Frenkel-Poole emission. This is justified by comparing the slopes of that two lines. This proves again that Frenkel-Poole emission is a reasonable assumption for $J_2(E_2)$.

B. Transient Analysis

The rate of change of charge stored at gold ion implanted trapping centers is proportional to the difference in current-density values for both regions of the implanted oxide at a given charging voltage v and time t,

$$\frac{dQ(v,t)}{dt} = J_2(v,t) - J_1(v,t) \qquad (8)$$

where Q is the stored charge per unit area, J_2 and J_1 are the current density in regions 2 and 1 of the oxide respectively. Both Q and J are function of applied voltage V and time t. The initial condition for induced trapped charge is determined by the past history of the device.

The room temperature computer solution of Eq.(8) with assumed zero initial stored charge are shown in Fig. 10. Also shown in the ordinate is the corresponding flat-band voltage V_{FB} . Experiment results for the induced charge in the oxide as a function of charging time are compared with computed solution in Fig. 11. The agreement between them is good.

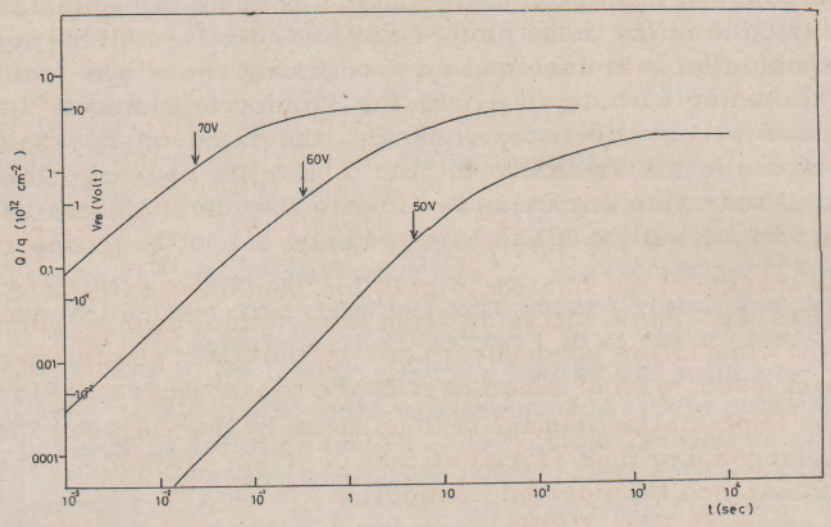

Fig.10. Computer solution of stored charge and the corresponding flatband voltage at room temperature as a function of time. The sample are similar to that used in Fig. 8. except that the oxide thickness is 720Å.

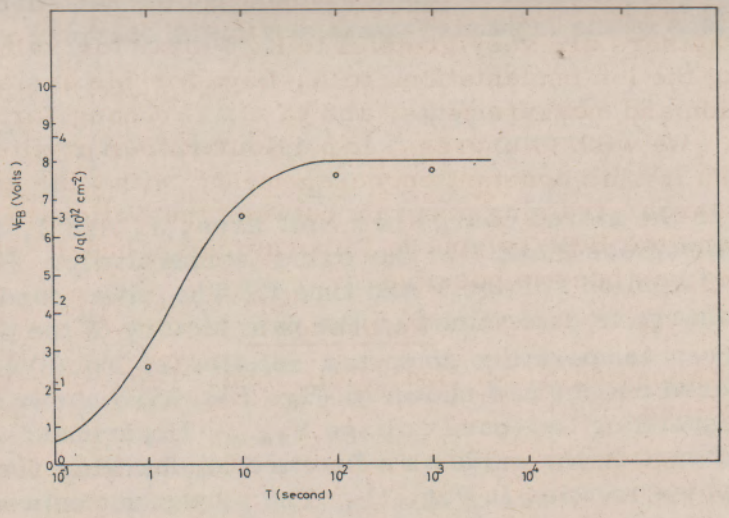

Fig. 11. The experimental results and the computer solution of stored charge as a function of time. A voltage of 60 Volts is applied at the alumimun dots. The oxide thickness is 720Å.

VII. Discussions and Conclusion

The gold ion implantation introduces both the fast interface states and the trapping centers in the oxide. The fast interface states depend strongly on the implanted gold dose and on the thickness of the oxide film. At 400°C annealing with dry nitrogen for 30 minutes, most of the fast interface states will be eliminated, and the effect of deep acceptor type trapping centers in the oxide due to gold ions will then have more important effect. If the oxide thickness is close to the ion projected range, the Si-SiO_2 interface will be highly damaged and cannot be easily removed.

The transport mechanism in gold ion implanted oxide MOS structure is due to Frenkel-Poole emission from the trapping levels which is 1.21 eV below the conduction band introduced by the ion implantation damage. The transport mechanism of inner part of the oxide where it is nearly free from ion implantation damage is dominated by Fowler-Nordheim tunneling. Charges are thus stored at the gold ion trapping centers in the oxide to balance the current conduction.

As shown in Fig. 10 the charging time response is slow even when the applying voltage is quite large. One can increase the charging response by reducing the oxide thickness and the implantation energy.

The description of the gold trapping centers in this paper is only qualitative, because the steady-state and transient solutions for charge transport in MOS structure do not require knowledge of the exact trap distibution [4].

Acknowledgement

The authors are very grateful to K. Pickar for valuable discussion and doing the ion implantation, to A. Loya for his assistance in sample fabrication and measurements, and to C. Y. Chang for his helpful discussion. We wish to express, in particular, our gratitude to Professor L. J. Chu for his constant encouragement; with his enthusiastic help the research training program between the National Chiao Tung University and the Bell Telephone Laboratories, under which this work was done, has become possible.

References

1. D. Kahng and S. M. Sze, Bell Syst. Tech. J., Vol. 4; P. 1288, July-Aug. 1967.
2. J. T. Wallmark and T. H. Scott, RCA Review, Vol. 30, p. 335, June 1969.
3. E. C. Ross and J. T. Wallmark, RCA Review, Vol. 30, p. 366, June 1969.
4. D. Frohman-Bentchkowsky and M. Lenzlinger, J. of apple. Physics, Vol. 40, No. 8, P. 3307, July 1969.

5. F. A. Sewell, Jr. H. A. R. Wegener, and E. T. Lewis, Appl. Phys. Letters., Vol. 14, No. 2, p. 45, Jan. 1969.

6. N. J. Chou and B. L. Corwder, J. of Appl. Physics, Vol. 41, No. 4, p, 1731, March 1970.

7. Private communication with K. Pickar of Bell Labs., Murray Hill, N. J.U.S.A..

8. A. Goetzberger, Bell Syst. Tech. J., Vol. 45, p. 1097, 1966.

9. S. R. Hofstein and G. Warfield, Solid-Atate Elect., Vol. 8, p. 321, 1965.

10. E. H. Nicollian and A. Goetzberger, IEEE Trans. On E-D p. 108, March 1965.

11. M. Lenzlinger and E. H. Snow, J. Appl. Phys., Vol. 40, p. 278, 1969.

12. S. M. Sze, " Physics of Semiconductor Devices ", Table 9.4, p. 496